Virology 385 (2009) 496–504

Contents lists available at ScienceDirect

Virology

journal homepage: www.elsevier.com/locate/yviro

AcMNPV EXON0 (AC141) which is required for the efficient egress of budded virus nucleocapsids interacts with β-tubulin

Minggang Fang [a], Yingchao Nie [a], David A. Theilmann [a,b,*]

[a] Plant Science, Faculty of Land and Food Systems, University of British Columbia, Vancouver, B.C., Canada V6T 1Z4
[b] Pacific Agri-Food Research Centre, Agriculture and Agri-Food Canada, Box 5000, Summerland, B.C., Canada V0H 1Z0

ARTICLE INFO

Article history:
Received 28 October 2008
Returned to author for revision
15 November 2008
Accepted 8 December 2008
Available online 19 January 2009

Keywords:
AcMNPV
AC141
Exon0
Baculovirus
Viral egress
Microtubules

ABSTRACT

The *Autographa californica* multiple nucleopolyhedrovirus (AcMNPV) encoded protein, EXON0 (AC141), is required for the efficient transport of nucleocapsids out of the nucleus for the production of budded virus (BV). To further elucidate the molecular mechanisms by which EXON0 regulates BV production, EXON0 was tagged at the N-terminus with 3× FLAG–6× His. Protein complexes were isolated by tandem affinity purification and potential EXON0 specific interacting protein partners were gel purified and identified by LC–MS/MS. This analysis showed that the cellular protein, β-tubulin, co-purified with EXON0 which was confirmed by co-immunoprecipitation. In addition, immunofluorescence showed that EXON0 and β-tubulin co-localized during virus infection. The microtubule inhibitors colchicine and nocodazole were used to treat AcMNPV infected Sf9 cells and results showed that BV production was reduced by over 85%. These data suggest that the egress of AcMNPV budded virus may be facilitated by the interaction of EXON0 with β-tubulin and microtubules.

Introduction

Autographa californica multiple nucleopolyhedrovirus (AcMNPV), the archetype of the *Baculoviridae*, has a 133.9 kbp genome and encodes 154 predicted genes of 50 amino acids or greater. *Exon0* (*orf141*) is a conserved gene found in all lepidopteran baculoviruses of the genus *alphabaculovirus*. The deletion of *exon0* reduces the level of BV production up to 99% and the infection of Sf9 cells with an *exon0* knockout (KO) virus is restricted to a single cell or a few neighbouring cells. However, viral replication and polyhedra production are unaffected, suggesting that *exon0* plays a key role specific to BV production pathway (Dai et al., 2004). EXON0 is a structural component of both BV and ODV that localizes to the nucleocapsid fraction. Electron microscopy has also revealed that EXON0 is required for efficient transport of progeny nucleocapsids from the nucleus to the cytoplasm (Fang et al., 2007).

Baculovirus BVs enter insect and mammalian cells *via* adsorptive endocytosis (Hefferon et al., 1999; Volkman and Goldsmith, 1985). The acidification of late endosomes activates the fusogenicity of GP64 and results in the fusion of the viral and endosomal membranes (Blissard and Wenz, 1992; Leikina et al., 1992; Long et al., 2006). After the nucleocapsids are released from the endosomes, the incoming nucleocapsids induce the formation of thick transient actin bundles which appear to facilitate the transport of nucleocapsids to the nucleus (Charlton and Volkman, 1991, 1993; Lanier and Volkman, 1998). After the entry into the nucleus, viral transcription and DNA replication occur in a cascade-like fashion. At late times post infection, the progeny nucleocapsids are assembled in the virogenic stroma, transported out of the nucleus and bud at the cytoplasmic membrane to become BV. At very late times post infection, the progeny nucleocapsids are retained in the nucleus, enveloped by a virally induced intranuclear membrane and finally occluded into polyhedra to form ODV (Williams and Faulkner, 1997). The mechanism by which the nucleocapsids are shuttled so that they are destined to become BV or retained in the nucleus to become ODV is unknown. Also poorly understood is how nucleocapsids are transported from the nucleus to the plasma membrane but our results have shown that EXON0 is required for this process (Fang et al., 2007).

Microtubules are key components in the cytoskeleton of eukaryotic cells and play an important role in organelle transport, cell shape maintenance, mitosis, motility, and cell division (Jordan and Wilson, 2004). Microtubules are highly dynamic polymers of heterodimers of α- and β-tubulin, arranged parallel to a cylindrical axis to form tubes of 24 nm diameter that may be many micrometers long. Microtubules have long been implicated in viral nucleocapsid movement since their close association was first observed by electron microscopy (Granados, 1978; Luftig and Weihing, 1975). In the last decade, the involvement of microtubules in virus transport has been reported for a number of viruses (Carter et al., 2003; Funk et al., 2004; Lakadamyali et al., 2003; McDonald et al., 2002; Pelkmans et al., 2001; Seisenberger et al., 2000;

* Corresponding author. Pacific Agri-Food Research Centre, Agriculture and Agri-Food Canada, Box 5000, Summerland, B.C., Canada V0H 1Z0. Fax: +1 250 494 6415.
E-mail address: TheilmannD@agr.gc.ca (D.A. Theilmann).

0042-6822/$ – see front matter.
doi:10.1016/j.virol.2008.12.023

Sodeik et al., 1997; Suomalainen et al., 1999). In addition, quite a few specific viral proteins that interact directly with microtubules or with microtubule motor proteins have also been identified (Alonso et al., 2001; Elliott and O'Hare, 1998; Martin et al., 2002; Nejmeddine et al., 2000; Ogino et al., 2003; Ward and Moss, 2004).

To further dissect how EXON0 plays its critical role in the viral egress part of the viral infection cycle the objective of this study was to identify additional proteins with which EXON0 interacts. Using 3× FLAG–6× His tandem affinity purification (TAP) and LC–MS/MS the cellular protein β-tubulin was shown to associate with EXON0. This interaction was confirmed using co-immunoprecipitation, confocal microscopy and microtubule inhibitor drugs. These results suggest that microtubules may play an important role in BV production and their association with EXON0 may facilitate the transport of nucleocapsids from the nucleus to the plasma membrane.

Results

Construction of virus expressing TAP tagged EXON0

EXON0 has been shown to be required for the high level production of BV and for the efficient egress of nucleocapsids from the nucleus to the cytoplasmic membrane (Dai et al., 2004; Fang et al., 2007). To investigate the molecular basis for these observations and to better characterize the function of EXON0, we attempted to identify cellular binding partners. We used tandem affinity purification (TAP) coupled with LC–MS/MS protein identification as it has been shown to be very successful in and highly sensitive in identifying protein–protein interactions (Puig et al., 2001; Rigaut et al., 1999).

The 3× FLAG–6× His TAP tag has been shown to be very efficient for purifying protein complexes in insect cells and was used in this study (Yang et al., 2006). The *exon0*KO bacmid bMON14272 *exon0*KO was repaired by a fusion construct of EXON0 in which the 3× FLAG–6× His TAP tag was fused at the N-terminus of EXON0 (Fig. 1A). The titer produced by *exon0*KO-3× FLAG–6× His-HA-EXON0 (3.3×10^8 $TCID_{50}$/ml) at 96 h post infection (hpi) was similar to *exon0*KO-HA-EXON0 indicating that the addition of the TAP tag did not affect the function of EXON0 and the fusion protein could fully rescue the KO bacmid. The fusion protein was detected at the correct size by western blot (Data not shown).

Identification of β-tubulin as an interacting partner of EXON0

Sf9 cells were infected with *exon0*KO-3× FLAG–6× His-HA-EXON0 or the control virus *exon0*KO-HA-EXON0 and protein complexes were isolated at 24 hpi using 3× FLAG–6× His TAP and the results are shown

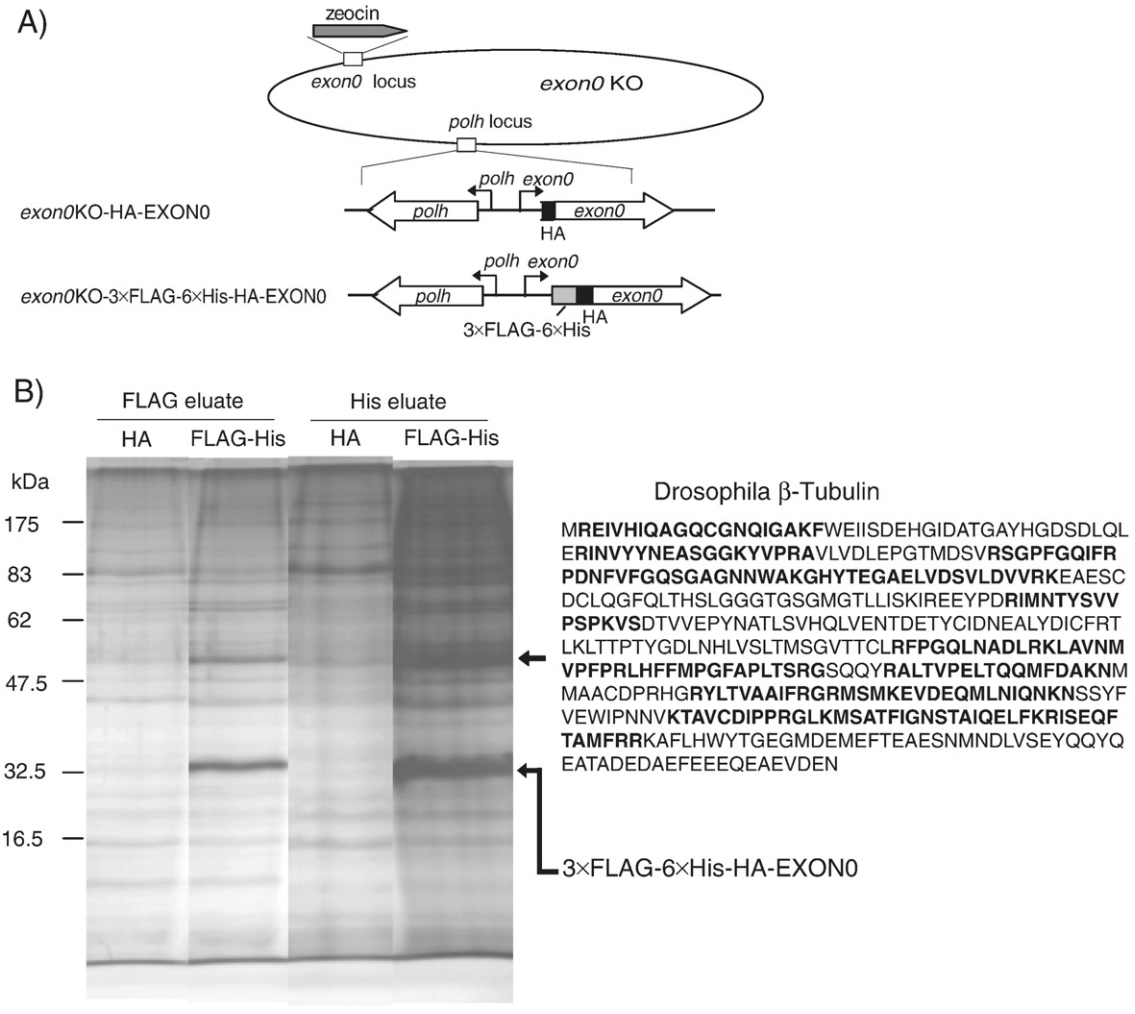

Fig. 1. Identification of β-tubulin as an interacting partner of EXON0. (A). Schematic diagrams of bacmid viruses that express EXON0 fusion proteins, *exon0*KO-3× FLAG–6× HIS-HA-EXON0 and *exon0*KO-HA-EXON0 that fused the TAP tag 3× FLAG–6× His-HA or just the HA epitope tag at the N-terminal of EXON0. (B). TAP complexes associated tagged EXON0 proteins. Sf9 cells were infected with the *exon0*KO-3× FLAG–6× His-HA-EXON0 (FLAG-His) or *exon0*KO-HA-EXON0 (HA) and harvested at 24 hpi and subjected to affinity purification. Complexes were separated by SDS-PAGE after the single affinity purification (FLAG eluate) and double affinity purification (His eluate) followed by silver staining (see Materials and methods). The β-tubulin specific band (top arrow) was identified by LC–MS/MS. The *Drosophila* β-tubulin sequence is shown on the right and the bold residues of β-tubulin represent the peptide fragments of β-tubulin identified by LC–MS/MS.

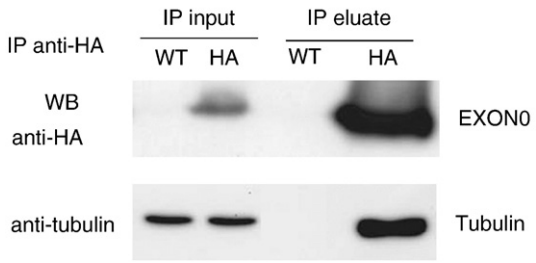

Fig. 2. Co-immunoprecipitation of EXON0 and β-tubulin. Sf9 cells were infected with WT AcMNPV or *exon0*KO-HA-EXON0 (HA) and cells were harvested at 24 hpi and subjected to co-immunoprecipitation. Samples were separated by 10% SDS-PAGE and analyzed by western blot. For input 0.125% of the total cell lysate was loaded, and 5% of the immunoprecipitation (IP) eluate was loaded. The antibody used for the western blots (WB) is shown on the left.

in Fig. 1B. One clear specific band of approximately 50 kDa was observed from *exon0*KO-3× FLAG–6× His-HA-EXON0 infected cells compared to cells infected with the control *exon0*KO-HA-EXON0 virus, The 50 kDa band was excised and subjected to LC–MS/MS for protein identification. It was determined that there were significant homologies between this protein and the *Drosophila* cytoskeletal protein β-tubulin (GenBank AAO24999).

Co-immunoprecipitation analysis of EXON0 and β-tubulin

To confirm the physical association between EXON0 and β-tubulin, we performed co-immunoprecipitation studies. Sf9 cells were infected with *exon0*KO-HA-EXON0 or with AcMNPV wild type (WT) (strain E2) which does not express an HA epitope tagged EXON0. Protein complexes immunoprecipitated with anti-HA agarose beads were examined by Western blot (Fig. 2). The results showed that β-tubulin was detected from the eluate of *exon0*KO-HA-EXON0 infected cells, but not from AcMNPV WT infected cells (Fig. 2). This result agrees with the TAP results and supports the conclusion that EXON0 interacts with β-tubulin either directly or in a complex.

Co-localization of EXON0 and β-tubulin

To further investigate the association of EXON0 with β-tubulin, co-localization studies were performed using confocal microscopy. Sf9 cells were infected with *exon0*KO-HA-EXON0 and fixed at 24 hpi. In infected cells, intense fluorescence is observed showing the localization of EXON0 in the ring zone in the nucleus and also in the cytoplasm heavily concentrated against the plasma membrane consistent with previous observations (Fang et al., 2007) (Fig. 3A). The β-tubulin antibody detected microtubule structures from uninfected Sf9 cells that predominantly extend from the perinuclear region to the cytoplasmic periphery with very little in the nucleus (Fig. 3A). In infected Sf9 cells at 24 hpi microtubules were predominantly detected in the cytoplasmic fraction. In addition, microtubules were also detected at higher levels in the infected nucleus localizing to the virogenic stroma. This suggested that AcMNPV infection induces reorganization or increased formation of microtubules within the nucleus similar to what has been reported for actin (Charlton and Volkman, 1991). EXON0 showed strong general co-localization with microtubules in the cytoplasm but weaker co-localization in the nucleus.

In Sf9 cells the co-localization of EXON0 with microtubules was consistent but relatively general and it was difficult to determine if there was specific association with individual microtubule fibres. To clearly visualize the microtubule network a more fibroblastic cell type, Tn-5b1, was used to confirm the co-localization of EXON0 and β-tubulin. Analysis of the uninfected Tn-5b1 cells showed that the network of microtubules structures were clearly visualized (Fig. 3B). After infection with *exon0*KO-HA-EXON0 at 24 hpi, many cells rounded up and the cytoplasmic volume decreased. However in a significant number of cells the microtubule networks remain visible and can be clearly observed at 24 and 48 hpi. At 24 hpi when the rate of BV production is exponential, EXON0 is observed in both the nucleus and cytoplasm of Tn-5b1 cells but in a more distributed pattern than in Sf9 cells. Merging of the EXON0 and Tubulin images shows that significant co-localization occurs at 24 hpi, both in the nucleus and in cytoplasm and even into the cytoplasmic extensions (Fig. 3B enlarged). At 48 hpi, after BV production has levelled off, infected Tn-5b1 cells became rounder with fewer cytoplasmic extensions and the microtubule filaments became shortened. Interestingly there is less co-localization between the microtubules and EXON0 in the nucleus but it is still observed along microtubules in the cytoplasm particularly at the cell periphery (Fig. 3B 48 hpi, Enlarged).

BV production in the presence of microtubule inhibitors

The results described above suggest that EXON0's mechanism of action for BV production requires interaction with microtubules. Therefore disruption of microtubules could have a detrimental impact reducing BV production and disrupting EXON0 interaction. To test this possibility infection of Sf9 cells with *exon0*KO-HA-EXON0 was performed in the presence of colchicine or nocodazole which inhibit microtubule polymerization. At 72 hpi, the BV supernatants of treated and untreated cells were assayed by end point dilution and as shown in Fig. 4A in Sf9 cells, the BV production in the presence of colchicine or nocodazole showed reductions in titre that were dependent on the concentrations of colchicine or nocodazole. The titers of BV under 10 μM colchicine or 25 μM nocodazole showed reductions of 85.3% and 82.9% respectively compared to virus titres from untreated cells. The same experiment was also performed in Tn-5b1 cells (Fig. 4B) and the colchicine and nocodazole again reduced the BV production significantly. This was consistent with previously published results which showed that 10 μM colchicine reduced AcMNPV BV production by 75% in Sf9 cells (Volkman and Zaal, 1990). This result further supports the conclusion that microtubules and their dynamics play a role in AcMNPV BV production.

Co-localization of EXON0 with microtubules in the presence of microtubule inhibitors

To determine the affect of microtubule inhibitors on the co-localization of EXON0 and microtubules, their distribution in the presence of microtubule inhibitors was also examined by confocal microscopy. Sf9 cells were infected with *exon0*KO-HA-EXON0 in the presence of 10 μM colchicine and the co-localization of EXON0 and β-tubulin was monitored at 24 hpi (Fig. 5A). Comparison of the untreated and treated cells shows that in the presence of colchicine, microtubule integrity was impaired and showed significant depolymerization in the cytoplasm (Fig. 5A). Analysis of EXON0 localization in colchicine treated Sf9 cells shows that the double RING pattern of EXON0 in cytoplasm and nucleus was almost completely disrupted. Merging of the two images shows that co-localization of EXON0 and microtubules is reduced considerably which is clearly shown in the enlarged panels (Fig. 5A).

The colchicine experiment was repeated using Tn-5b1 cells due to the improved microtubule resolution (Fig. 5B). In Tn-5b1cells, the colchicine induced depolymerization of microtubules was more significant at 48 hpi than 24 hpi. Compared to the untreated infected cells the colchicine treatment resulted in the complete loss of microtubule network. Interestingly the distribution of EXON0 appeared to be significantly affected producing aggregates in the cytoplasm and the level in the nucleus was greatly reduced (Fig. 5B). Some co-localization was observed at the periphery of the EXON0 aggregates and randomly throughout the cytoplasm. These results

indicate that β-tubulin and the integrity of microtubules is required for the normal distribution of EXON0 during infection.

EXON0 domains required for association with β-tubulin

To determine if a specific domain of EXON0 required for the association with β-tubulin, Sf9 cells were infected with viruses that express point mutants of HA tagged EXON0 that have been previously described (Fang et al., 2008). To enable high enough expression levels of the non-functional mutant proteins they have to be expressed from a bacmid that produces untagged WT EXON0. After co-immunoprecipitation (Fig. 6), β-tubulin was detected with EXON0-HA, L157/A and C231C232/AA mutants but F44F46M49, K59R65/AA, V64F69I72/AAA, H113/A, V141V143L148/AAA reduced the association with β-tubulin. The mutants C111/A, I116I122I126/AAA, L155F162I169/AAA, V176L190/AA and L190/P abolished the β-tubulin association, suggesting these conserved residues are critical for the association with β-tubulin. At least one mutant in each domain, with the exemption of the RING domain, appeared to have a significant impact on β-tubulin interaction suggesting they are all required for β-tubulin interactions.

Discussion

How the nucleocapsids of lepidopteran baculoviruses are transported from the nucleus to the plasma membrane to form BV is an essential part of the baculovirus life cycle for which many aspects remain unresolved. One component that is involved in the egress pathway is EXON0 (AC141), a conserved structural protein of BV nucleocapsids found in all lepidopteran alphabaculoviruses and is required for the efficient egress of nucleocapsids from the nucleus (Fang et al., 2007). In this study we have used a TAP-tag to identify a cellular protein, β-tubulin, that interacts with EXON0 suggesting a possible interaction with microtubules. EXON0 interaction with β-tubulin was confirmed by co-immunoprecipitation and

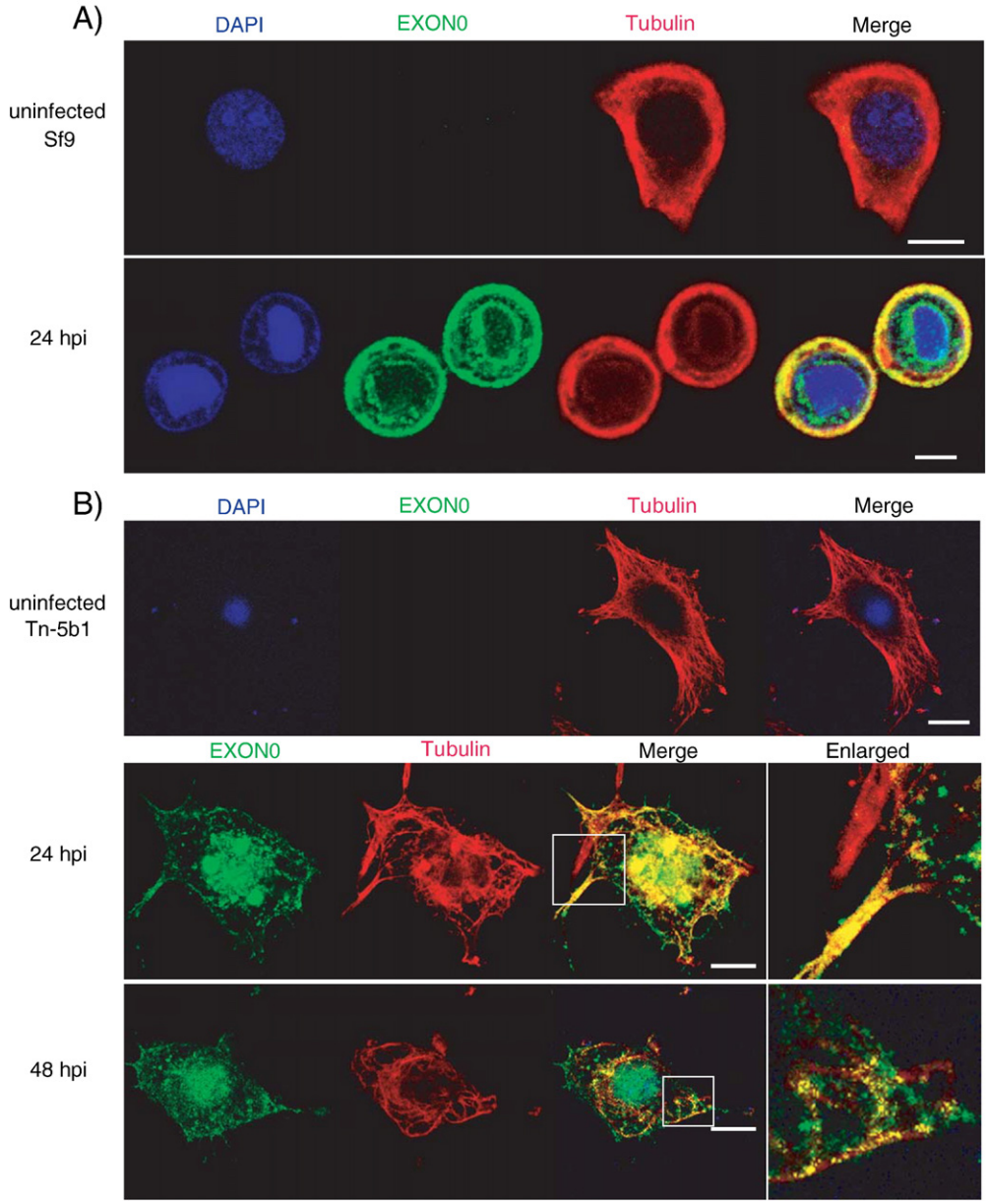

Fig. 3. Co-localization of EXON0 with β-tubulin and microtubules in infected cells. (A) Sf9 or (B) Tn-5b1 cells were infected with *exon0*KO-HA-EXON0 and fixed at 24 and 48 hpi. EXON0 was detected with a rabbit polyclonal anti-HA antibody and with Alexa 488 conjugated goat anti-rabbit IgG. Microtubules and tubulin were detected with a mouse anti-β-tubulin monoclonal antibody and Alexa 635 conjugated goat anti-mouse IgG. Cells were visualized by fluorescence confocal microscopy. For Sf9 cells (A) cells were also stained with DAPI for nuclear visualization. The white square in (B) in the merged image is the area enlarged on the right. Bars, 10 μm.

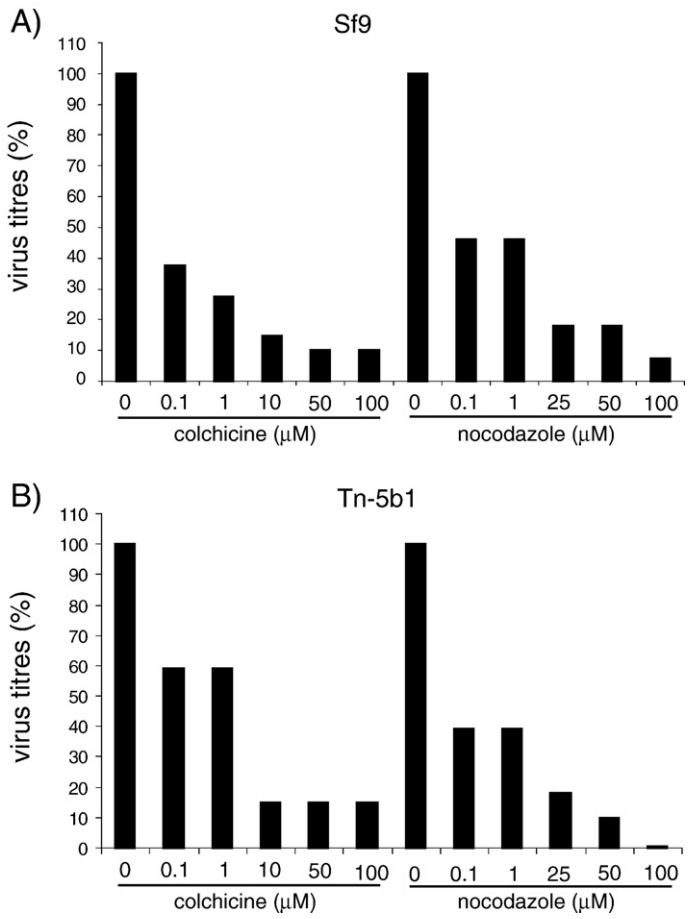

Fig. 4. Microtubule inhibitors reduce BV production. Sf9 cells or Tn-5b1 cells were infected with *exon0*KO-HA-EXON0 in the presence of the microtubule inhibitors colchicine (0, 0.1, 1, 10, 100 and 500 μM) or nocodazole (0, 0.1, 1, 25, 100 and 500 μM) at an MOI of 10. Supernatants were harvested at 72 hpi and viral titres were determined by end point dilution assay. The experiment shown was done in duplicate and the average titres are presented as the percentage of untreated control values.

confocal immunofluorescence microscopy which showed co-localization with microtubules in infected cells (Figs. 2 and 3).

The subtle microtubule network structure was more clearly visualized with Tn-5B1 cells using immunofluorescence confocal microscopy and co-localization of EXON0 with microtubules could be observed, particularly at regions of the plasma membrane and in some of the cytoplasmic extensions. At 24 hpi there was also significant co-localization in the nucleus but it was greatly reduced by 48 hpi. As EXON0 is a nucleocapsid protein, its co-localization with microtubules supports the concept that microtubules are being utilized for nucleocapsid egress.

Viruses are dependent on the machinery of the cell for both trafficking and transport as they are obligate intracellular parasites. As nucleocapsids are very large structures, often greater than 500 kDa or 50 nm in length, their free diffusion is restricted in the cytoplasm (Seksek et al., 1997; Stidwell and Greber, 2000). To overcome this barrier viruses have developed transport mechanisms that are based on microtubules. This strategy is common and has been employed by many diverse groups of viruses (reviewed by Dohner et al, 2005). The transport of baculovirus nucleocapsids on microtubules is therefore a potential mechanism for facilitating nucleocapsid egress from the nucleus to the plasma membrane.

The microtubule inhibitors colchicine and nocodazole demonstrated that microtubule dynamics and integrity have a significant impact on BV production. These drugs inhibit polymerization of Sf9 and Tn-5B1 microtubules and caused nearly a log (85%) reduction in BV yield compared to untreated cells (Fig. 4). Volkman and Zaal (1990) reported a 0.6 log (75%) reduction in BV production in Sf21 cells treated with 10 μM colchicine and a delay and decrease in titre in cells treated with taxol but no role for microtubules was attributed for virus production. The titres were similar in drug treated and non-treated Sf9 cells at 24 and 48 hpi (Data not shown), which is also comparable to results reported Volkman and Zaal (1990), suggesting significant microtubule disruption is required to inhibit BV production. The effect of microtubule inhibitors on AcMNPV BV production was not as great as deleting EXON0, however the drug treatments do not cause a complete depolymerization of the microtubule cytoskeletal structures (Fig. 5). The surviving structures could provide limited transport of nucleocapsids accounting for the reduced level of BV observed. Similar to the results of this study incomplete depolymerization of microtubules is also observed in mammalian cells when treated with nocodazole. Nevertheless reduced infection levels or a 60–85% reduction in extracellular virus yield is observed in cells infected with viruses known to utilize microtubules (Alonso et al., 2001; Das et al., 2006; Naranatt et al., 2005; Ploubidou et al., 2000; Sodeik et al., 1997)

As indicated above we showed that AcMNPV infection resulted in increased levels of β-tubulin and microtubules in the nucleus (Fig. 3) a finding that has also been reported by Carpentier et al. (2008). Reorganization of cytoplasmic microtubules due to virus infection was also reported by Volkman and Zaal (1990). Although microtubules are generally thought of as cytoplasmic structures during interphase, nuclear tubulins and microtubules have been observed in many cell lines and form during the M phase of the cell cycle (Menko and Tan, 1980; Ovechkina et al., 2003; Walss-Bass et al., 2002; Yeh and Ludueña, 2004). In addition, some highly conserved eukaryotic kinesin-related motor proteins operate specifically in the nucleus (Hildebrandt and

Hoyt, 2000). Interestingly it is known that AcMNPV infection induces cell cycle arrest at G2/M phase (Belyavskyi et al., 1998; Braunagel et al., 1998) creating an environment that favours not only DNA replication, but potentially, the nuclear organization of microtubules. The presence of nuclear microtubules in AcMNPV infected cells could therefore support nucleocapsid movement to the inner nuclear membrane from the virogenic stroma (Fig. 7).

How EXON0 associates with β-tubulin and microtubules in infected cells still remains to be determined. Our mutation analysis (Fig. 6) did not identify any specific domain of EXON0 required for this interaction. Using the *Drosophila melanogaster* cDNAs of α- and β-tubulin, we investigated if EXON0 binds tubulin directly via yeast two hybrids (data not shown). The negative result, though not surprising, suggests that EXON0 binds α- or β-tubulin and microtubules indirectly via other viral or cellular proteins. A number of viral proteins in other systems utilize motor proteins for anterograde transport on microtubules to the cell periphery. This usually requires kinesin motors which, in humans, encompass a super family of 45 members (Caviston and Holzbaur, 2006). Cargo that is transported by kinesin motors usually interacts indirectly via scaffolding or adaptor proteins (Caviston and Holzbaur, 2006). However, viral proteins for the most part appear to interact directly with kinesin subunits, such as the HSV US11 tegument protein (Diefenbach et al., 2002; Dohner et al., 2005). US11 interacts with conventional kinesin heavy chain and plays a major role in the anterograde transport of nucleocapsids on microtubules in axons. Whereas the vaccinia virus A36R protein facilitates virion microtubule movement by binding to kinesin light chains (Ward and Moss, 2004). Further studies will be done to determine if EXON0 or other baculoviral proteins associate with kinesin.

Previous electron microscopy data (Granados and Lawler, 1981; Williams and Faulkner, 1997) have suggested a pathway for baculovirus nucleocapsid egress that can be dissected into six general steps

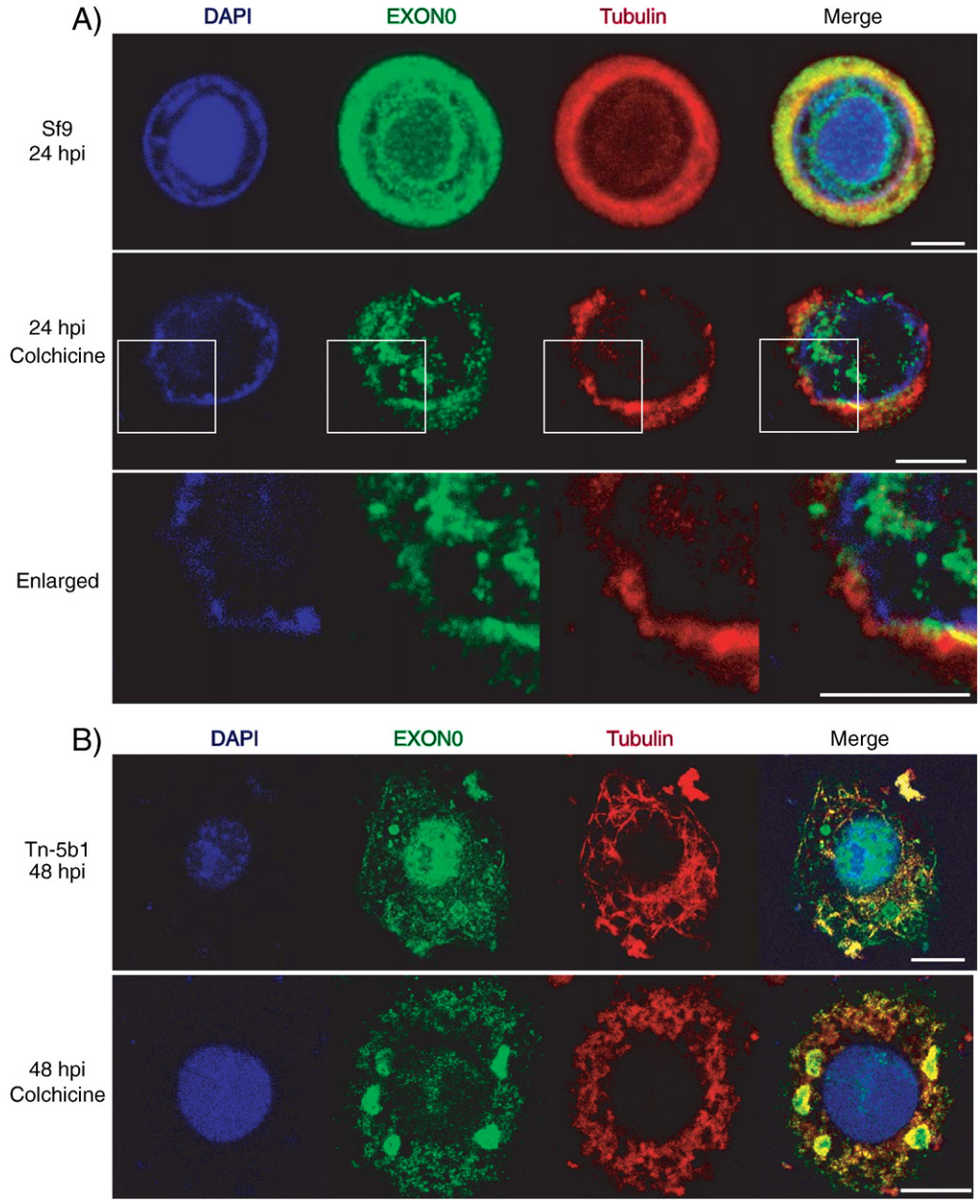

Fig. 5. Co-localization of EXON0 with β-tubulin and microtubule in infected cells in the presence of colchicine. (A) Sf9 cells and (B) Tn-5b1 were treated without or with 10 μM colchicine and infected with *exon0*KO-HA-EXON0 and immunofluorescence confocal microscopy was performed at 24 or 48 hpi as described in Fig. 3 for detection of EXON0 and β-tubulin. For nuclear localization the cells were also stained with DAPI. The white square in 24 hpi colchicine (A) is the area enlarged and shown in the third row of images (Enlarged). Bars, 10 μm.

(Fig. 7). These are (1) transport of nucleocapsids in the nucleus from the virogenic stroma to the nuclear envelope; (2) envelopment of the nucleocapsids in a nuclear membrane and movement through the nuclear envelope; (3) formation of vesicles in the cytoplasm; (4) nuclear membrane-derived vesicle is lost and naked nucleocapsids are found in the cytoplasm; (5) nucleocapsids migrate to the plasma membrane; and (6) nucleocapsids bud from the plasma membrane. Our data adds to this model and suggests that EXON0 facilitates the interaction of BV nucleocapsids and microtubules enabling the efficient transport of nucleocapsids in Step 1 and Step 5 of the egress pathway (Fig. 7). Electron microscopy has also shown the close association of nucleocapsids with apparent microtubules (Granados, 1978; Granados and Lawler, 1981). To confirm aspects of this model future work will be required to determine the nature of EXON0 interaction with β-tubulin and microtubules.

Materials and methods

Cells and viruses

Spodoptera frugiperda Sf9 cells and *Trichoplusia ni* cells (BTI-Tn-5b1) (Granados et al., 1994) were maintained in 10% foetal bovine serum-supplemented TC100 medium at 27 °C. AcMNPV recombinant bacmids were derived from the commercially available bacmid bMON14272 (Invitrogen Life Technologies) and propagated in *Escherichia coli* strain DH10B. The WT virus used was AcMNPV strain E2.

Construction of 3× FLAG–6× His-tagged EXON0 and repaired virus

To tag EXON0 with 3× FLAG–6× His at the N-terminus for TAP, 3× FLAG–6× His tag was amplified with primer 1215 (5′- GCGGAGATC-TATGGACTACAAAGACCATGAC -3′) and 1216 (5′- GCGGAGATC-TGCTGCCGCGCGGCAC -3′) from pCaSpeR-hs-act-Tetra tag plasmid (Yang et al., 2006) and *exon0* was amplified using primers 1213 (5′-GCGGAGATCTTACCCCTACGACGTGCCC -3′) and 1214 (5′- GCGGA-GATCTGTTGCGTTGCCCGTTATC -3′) by inverse polymerase chain reaction (PCR) using p2ZeoKS-HA-exon0 (Fang et al., 2007) as a template. The two amplified linear fragments were digested by BglII, gel purified and ligated and transformed into DH5α competent cells. Correct clones were confirmed by restriction digestion and sequencing. The resulting plasmid was named p2Zeo-3× FLAG–6× His-HA-exon0. The correct plasmid construction of pHA-exon0 was confirmed by restriction digestion and sequencing.

To introduce *exon0* into bMON 14272 *exon0*KO, the rescue transfer vector was constructed using the plasmid backbone pFAcT (Dai et al., 2004). pFAcT contains two Tn*7* transposition excision sites that allow the genes cloned between the sites to be transposed into the mini ATT region located in the AcMNPV bacmid. p2Zeo-3× FLAG–6× His-HA-exon0 was digested with XhoI and XbaI. The excised fragment, containing the native late promoter of *exon0*, 3× FLAG–6× His-HA-exon0 and an OpMNPV *ie1* poly(A), was cloned into the XhoI and XbaI sites of pFAcT to generate pFAcT-3× FLAG–6× His-HA-exon0. In addition to the cloned gene of interest, the pFAcT backbone contains AcMNPV *polyhedrin*, which is included in the transposed DNA cassette. The recombinant AcMNPV bacmids containing the 3× FLAG–6× His-HA-exon0 was generated by Tn*7*-mediated transposition as previously described (Luckow et al., 1993). The repaired virus was named *exon0*KO-3× FLAG–6× His-HA-EXON0. Virus stock was prepared and titered.

3× FLAG–6× His TAP and protein identification

Sf9 cells (3×10^8) were infected with *exon0*KO-3× FLAG–6× His-HA-EXON0 or control virus *exon0*KO-HA-EXON0 (Fang et al., 2007) at a multiplicity of infectivity (MOI) of 10. The affinity purification method was adapted from Yang et al. (2006). At 24 hpi cells were harvested and washed with phosphate buffered saline (PBS, 137 mM NaCl, 10 mM phosphate, 2.7 mM KCl, pH 7.4), centrifuged at 800 *g* for 5 min. Cells were resuspended in 2 ml lysis buffer (15 mM HEPES pH 7.6, 10 mM KCl, 0.1 mM EDTA, 0.5 mM EGTA,1 mM DTT, 1% proteinase inhibitor cocktail (Sigma)), passed twice through a French press at 8.27 MPa (1000 psi) at 4 °C. The cell lysate was centrifuged at 18,000 *g* for 10 min and the supernatant was transferred to equilibrated anti-FLAG M2 affinity beads (Sigma) and incubated overnight at 4 °C on an orbiting platform. The beads were then transferred to Bio-Rad mini-columns, washed once with 1 ml cold lysis buffer and 6 times with 1 ml TBS buffer (50 mM HEPES, pH 7.6, 150 mM NaCl, 0.1% Triton). Protein was eluted from the FLAG affinity beads with 500 μL of 300 μg/mL 3× FLAG peptide (Sigma) in TBS. The FLAG eluate was incubated with 50 μL Talon cobalt resin (BD Biosciences Clontech) for 1 h at 4 °C. The resin was washed 4 times with 1 ml TBS and eluted with 300 μL TBS containing 300 mM imidazole. The eluate was vacuum concentrated to 80 μL, mixed with 80 μL 2× protein sample buffer (PSB, 0.25 M Tris–Cl, pH6.8, 4% SDS, 20% glycerol,10% 2-mercaptoethanol, 0.02% bromophenol blue), boiled at 100 °C for 5 min, subjected to sodium dodecyl sulfate polyacrylamide gel electrophoresis (SDS-PAGE), silver staining and western blot. Protein bands specific to the 3× FLAG–6× His-HA-EXON0 were cut from the gel, subjected to in-gel digestion and identified by Liquid Chromatography Mass Spectrometry/Mass

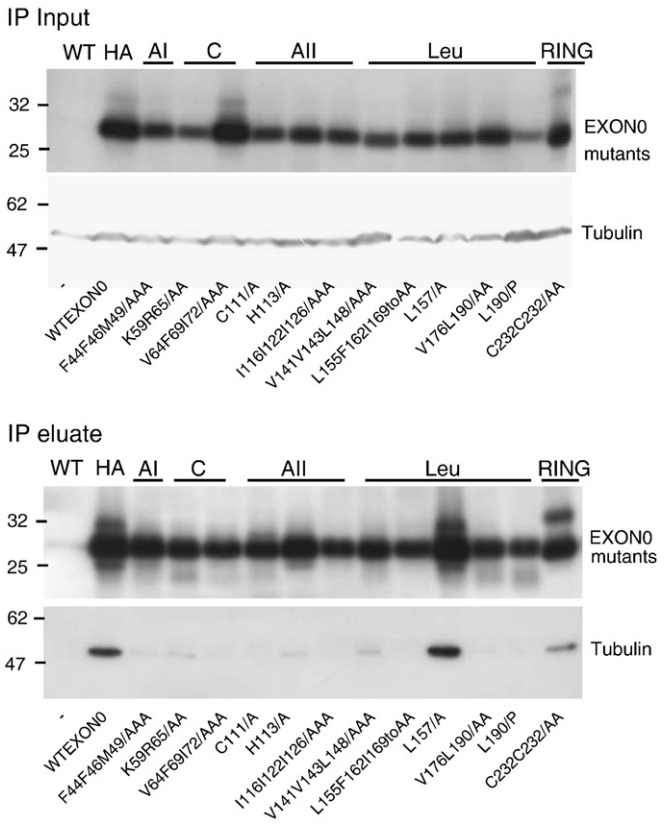

Fig. 6. Co-immunoprecipitation of EXON0 point mutants and β-tubulin. The ability of EXON0 point mutants to co-immunoprecipitate β-tubulin was examined by infecting Sf9 cells with the AcMNPV bacmid AcBac (WT), AcBac expressing EXON0-HA, or 12 point mutants of EXON0-HA (Fang et al., 2008). The point mutants are located in the acidic I (AI), Charged (C), acidic II (AII), leucine zipper (Leu) or RING domains of EXON0. At 24 hpi, cells were collected and lysed for immunoprecipitation (IP). Each lane of the upper panel, IP input, represents 0.125% of the total cell lysate. After immunoprecipitation with anti-HA antibodies, 10% of the total immunoprecipitation eluate were analysed by Western blot (lower panel, IP eluate) using anti-HA, anti-β-tubulin antibodies.

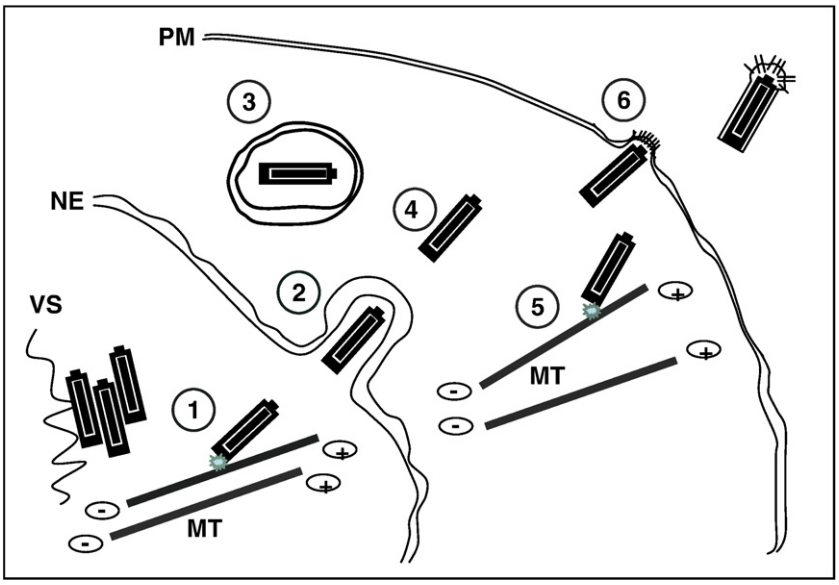

Fig. 7. Model for the role of EXON0 and microtubules in the egress pathway of BV nucleocapsids. The egress of nucleocapsids in BV pathway compromises of six major steps (Granados and Lawler, 1981; Williams and Faulkner, 1997). (1) Transport of nucleocapsids from the virogenic stroma to the inner nuclear membrane, (2) transit of nucleocapsids through the nuclear envelope, (3) formation of nucleocapsids containing vesicles in the cytoplasm, (4) de-envelopment of nucleocapsids, (5) migration of naked nucleocapsids to plasma membrane, (6) budding of nucleocapsids from the plasma membrane. It is proposed that EXON0 facilitates the interaction of nucleocapsids and microtubules for the efficient transport of nucleocapsids to nuclear and plasma membranes in Step 1 and step 5 of BV pathway. VS, virogenic stroma; NE, nuclear envelope; MT, microtubules; PM, plasma membrane.

Spectrometry (LC–MS/MS) at the Proteomics Core Facility of University of British Columbia.

Immunoprecipitation

Sf9 cells (2×10^8) were infected with either WT AcMNPV E2 or *exon0*KO-HA-EXON0 at a MOI of 10. Cells were lysed and subjected to immunoprecipitation as previously described (Fang et al., 2007). To identify the critical residues of EXON0 required for association with β-tubulin, Sf9 cells were infected with WT AcBac or WT AcBac expressing one of the point mutants of EXON0 (Fang et al., 2008), harvested at 24 hpi.

Immunofluorescence

Sf9 or Tn-5b1 cells were infected with *exon0*KO-HA-EXON0 using a MOI of 10. For the microtubule inhibitor treatment, colchicine (Sigma) and nocodazole (Sigma) were titrated in uninfected Sf9 and Tn-5b1 cells. Colchicine was effective at 10 μM in Sf9 cell and Tn-5b1 cells which resulted in cell rounding of over 99% but less 1% mortality after 24 h incubation. For immunofluorescence, cells were incubated with 10 μM colchicine (Sigma) throughout infection. At 24 and 48 hpi, the supernatant was removed and the cells were washed three times in PBS, followed by fixation with 4% paraformaldehyde for 15 min. The fixed cells were washed three times with PBS each for 10 min, permeabilized with 0.15% Triton X-100 for 15 min and were then blocked for 60 min in the blocking buffer (2% bovine serum albumin in PBS). Cells were incubated with rabbit polyclonal anti-HA antibody (1:200) (Abcam) and mouse monoclonal anti-β-tubulin antibody (1:200) (Abcam, TU06). The cells were washed three times for 10 min each time in blocking buffer, followed by 1 h incubation with Alexa 488-conjugated goat anti-rabbit IgG (1:500) (Molecular Probe) and Alexa 635-conjugated goat anti-mouse antibody (1:500) (Molecular Probes). Cells were subsequently washed three times for 10 min each time in PBS, followed by staining with 200 ng/ml DAPI (4′, 6′-diamidino-2-phenylindole) (Molecular Probes) and examined using a Leica confocal Microscope. The co-localization between EXON0 and microtubules was visualized with Imaris software (Bitplane).

Western blot analysis

The protein eluates from the 3× FLAG–6× His purification and co-immunoprecipitation were mixed with equal volumes of 2× sodium dodecyl sulfate PSB, and incubated at 100 °C for 5 min. Protein samples were separated by 10% SDS-PAGE and transferred to Millipore Immobilon-P membrane with the Bio-Rad Mini-Protean II. The membranes were probed with one of the following primary antibodies: (i) mouse monoclonal anti-HA antibody (Covance, HA11), 1:1000; (ii) mouse monoclonal β-tubulin antibody (Abcam, TU-06). Horseradish peroxidase-conjugated rabbit anti-mouse secondary antibody (1:15,000) was used with the Enhanced Chemiluminescence System (Amersham).

Production of budded virus in the presences of microtubule inhibitors

Sf9 cells or Tn-5b1 cells (1.0×10^6 cells/35 mm diameter well of a six-well plate) were infected with *exon0* KO-HA–EXON0 at MOI of 10 in 0.3 ml TC-100 media with gentle rocking for 1 h, then virus inoculum was removed. Cells were washed once with 1 ml TC-100 and incubated in 1.5 ml TC-100 at 27 °C. For microtubule drugs treatment, cells were incubated with 0, 0.1, 1, 10, 100 and 500 μM colchicine (Sigma) or 0, 0.1, 1, 25, 100 and 500 μM nocodazole (Sigma) for 4 h before infection and throughout the infection. BV titers at 72 hpi were analyzed by end point dilution method as previously described (Fang et al., 2007).

Acknowledgments

The authors like to thank Dr. Henry Krause for kindly providing the 3× FLAG–6× His TAP tag plasmid. This study was supported in part by funding from the Natural Sciences and Engineering Research Council and the Biocontrol Network.

References

Alonso, C., Miskin, J., Hernaez, B., Fernandez-Zapatero, P., Soto, L., Canto, C., Rodriguez-Crespo, I., Dixon, L., Escribano, J.M., 2001. African swine fever virus protein p54 interacts with the microtubular motor complex through direct binding to light-chain dynein. J. Virol. 75, 9819–9827.

Belyavskyi, M., Braunagel, S.C., Summers, M.D., 1998. The structural protein ODV-EC27 of *Autographa californica* nucleopolyhedrovirus is a multifunctional viral cyclin. Proc. Natl. Acad. Sci. U.S.A. 95, 11205–11210.

Blissard, G.W., Wenz, J.R., 1992. Baculovirus GP64 envelope glycoprotein is sufficient to mediate pH-dependent membrane fusion. J. Virol. 66 (11), 6829–6835.

Braunagel, S.C., Parr, R., Belyavskyi, M., Summers, M.D., 1998. *Autographa californica* nucleopolyhedrovirus infection results in Sf9 cell cycle arrest at G2/M phase. Virology 244, 195–211.

Carpentier, D.C.J., Griffith, C.M., King, L.A., 2008. The baculovirus P10 protein of *Autographa californica* nucleopolyhedrovirus forms two distinct cytoskeletal-like structures and associates with polyhedral occlusion bodies during infection. Virology 371 (2), 278–291.

Carter, G.C., Rodger, G., Murphy, B.J., Law, M., Krauss, O., Hollinshead, M., Smith, G.L., 2003. Vaccinia virus cores are transported on microtubules. J. Gen. Virol. 84, 2443–2458.

Caviston, J.P., Holzbaur, E.L., 2006. Microtubule motors at the intersection of trafficking and transport. Trends Cell Biol. 16 (10), 530–537.

Charlton, C.A., Volkman, L.E., 1991. Sequential rearrangement and nuclear polymerization of actin in baculovirus-infected *Spodoptera frugiperda* cells. J. Virol. 65, 1219–1227.

Charlton, C.A., Volkman, L.E., 1993. Penetration of *Autographa californica* nuclear polyhedrosis virus nucleocapsids into IPLB Sf 21 cells induces actin cable formation. Virology 197, 245–254.

Dai, X., Stewart, T.M., Pathakamuri, J.A., Li, Q., Theilmann, D.A., 2004. *Autographa californica* multiple nucleopolyhedrovirus *exon0* (*orf141*), which encodes a RING finger protein, is required for efficient production of budded virus. J. Virol. 78 (18), 9633–9644.

Das, S., Nayak, D., Zhou, Y., Pattnaik, A., 2006. Visualization of intracellular transport of vesicular stomatitis virus nucleocapsids in living cells. J. Virol. 80, 6368–6377.

Diefenbach, R.J., Miranda-Saksena, M., Diefenbach, E., Holland, D.J., Boadle, R.A., Armati, P.J., Cunningham, A.L., 2002. Herpes simplex virus tegument protein US11 interacts with conventional kinesin heavy chain. J. Virol. 76, 3282–3291.

Dohner, K., Nagel, C.H., Sodeik, B., 2005. Viral stop-and-go along microtubules: taking a ride with dynein and kinesins. Trends Microbiol. 13, 320–327.

Elliott, G., O'Hare, P., 1998. Herpes simplex virus type 1 tegument protein VP22 induces the stabilization and hyperacetylation of microtubules. J. Virol. 72, 6448–6455.

Fang, M., Dai, X., Theilmann, D.A., 2007. *Autographa californica* multiple nucleopolyhedrovirus EXON0 (ORF141) is required for efficient egress of nucleocapsids from the nucleus. J. Virol. 81 (18), 9859–9869.

Fang, M., Nie, Y., Dai, X., Theilmann, D.A., 2008. Identification of AcMNPV EXON0 (AC141) domains required for efficient production of budded virus, dimerization and association with BV/ODV-C42 and FP25. Virology 375, 265–276.

Funk, A., Mhamdi, M., Lin, L., Will, H., Sirma, H., 2004. Itinerary of hepatitis B viruses: delineation of restriction points critical for infectious entry. J. Virol. 78, 8289–8300.

Granados, R.R., 1978. Early events in the infection of *Hiliothis zea* midgut cells by a baculovirus. Virology 90 (1), 170–174.

Granados, R.R., G., L., C.G., D., K.A., M., 1994. A new insect cell line from *Trichoplusia ni* (BTI-Tn-5B1-4) susceptible to *Trichoplusia ni* single enveloped nuclear polyhedrosis virus. J. Invertebr. Pathol. 64, 260–266.

Granados, R.R., Lawler, K.A., 1981. *In vivo* pathway of *Autographa californica* baculovirus invasion and infection. Virology l08, 297–308.

Hefferon, K.L., Oomens, A.G., Monsma, S.A., Finnerty, C.M., Blissard, G.W., 1999. Host cell receptor binding by baculovirus GP64 and kinetics of virion entry. Virology 258, 455–468.

Hildebrandt, E.R., Hoyt, M.A., 2000. Mitotic motors in *Saccharomyces cerevisiae*. Biochim. Biophys. Acta 1496, 99–116.

Jordan, M.A., Wilson, L., 2004. Microtubules as a target for anticancer drugs. Nat. Rev., Cancer 4 (4), 253–265.

Lakadamyali, M., Rust, M.J., Babcock, H.P., Zhuang, X., 2003. Visualizing infection of individual influenza viruses. Proc. Natl. Acad. Sci. U.S.A. 100, 9280–9285.

Lanier, L.M., Volkman, L.E., 1998. Actin binding and nucleation by *Autographa california* M nucleopolyhedrovirus. Virology 243 (1), 167–177.

Leikina, E., Onaran, H.O., Zimmerberg, J., 1992. Acidic pH induces fusion of cells infected with baculovirus to form syncytia. FEBS Lett. 304 (2–3), 221–224.

Long, G., Pan, X., Kormelink, R., Vlak, J.M., 2006. Functional entry of baculovirus into insect and mammalian cells is dependent on clathrin-mediated endocytosis. J. Virol. 80 (17), 8830–8833.

Luckow, V.A., Lee, S.C., Barry, G.F., Olins, P.O., 1993. Efficient generation of infectious recombinant baculoviruses by site-specific transposon-mediated insertion of foreign genes into a baculovirus genome propagated in *Escherichia coli*. J. Virol. 67 (8), 4566–4579.

Luftig, R.B., Weihing, R.R., 1975. Adenovirus binds to rat brain microtubules *in vitro*. J. Virol. 16, 696–706.

Martin, A., O'Hare, P., McLauchlan, J., Elliott, G., 2002. Herpes simplex virus tegument protein VP22 contains overlapping domains for cytoplasmic localization, microtubule interaction, and chromatin binding. J. Virol. 76, 4961–4970.

McDonald, D., Vodicka, M.A., Lucero, G., Svitkina, T.M., Borisy, G.G., Emerman, M., Hope, T.J., 2002. Visualization of the intracellular behavior of HIV in living cells. J. Cell Biol. 159, 441–452.

Menko, A.S., Tan, K.B., 1980. Nuclear tubulin of tissue culture cells. Biochim. Biophys. Acta 629, 359–370.

Naranatt, P.P., Krishnan, H.H., Smith, M.S., Chandran, B., 2005. Kaposi's sarcoma-associated herpesvirus modulates microtubule dynamics via RhoA-GTP-diaphanous 2 signaling and utilizes the dynein motors to deliver its DNA to the nucleus. J. Virol. 79, 1191–1206.

Nejmeddine, M., Trugnan, G., Sapin, C., Kohli, E., Svensson, L., Lopez, S., Cohen, J., 2000. Rotavirus spike protein VP4 is present at the plasma membrane and is associated with microtubules in infected cells. J. Virol. 74, 3313–3320.

Ogino, T., Iwama, M., Ohsawa, Y., Mizumoto, K., 2003. Interaction of cellular tubulin with Sendai virus M protein regulates transcription of viral genome. Biochem. Biophys. Res. Commun. 311, 283–293.

Ovechkina, Y., Maddox, P., Oakley, C.E., Xiang, X., Osmani, S.A., Salmon, E.D., Oakley, B.R., 2003. Spindle formation in *Aspergillus* is coupled to tubulin movement into the nucleus. Mol. Biol. Cell 14 (5), 2192–2200.

Pelkmans, L., Kartenbeck, J., Helenius, A., 2001. Caveolar endocytosis of simian virus 40 reveals a new two-step vesicular-transport pathway to the ER. Nat. Cell Biol. 3, 473–483.

Ploubidou, A., Moreau, V., K., A., I., R., C., G., Way, M., 2000. Vaccinia virus infection disrupts microtubule organization and centrosome function. EMBO J. 19, 3932–3944.

Puig, O., Caspary, F., Rigaut, G., Rutz, B., Bouveret, E., Bragado-Nilsson, E., Wilm, M., Seraphin, B., 2001. The tandem affinity purification (TAP) method: a general procedure of protein complex purification. Methods 24, 218–229.

Rigaut, G., Shevchenko, A., Rutz, B., Wilm, M., Mann, M., Seraphin, B., 1999. A generic protein purification method for protein complex characterization and proteome exploration. Nat. Biotechnol. 10, 1030–1032.

Seisenberger, G., Ried, M.U., Endress, T., Buning, H., Hallek, M., Brauchle, C., 2000. Real-time single-molecule imaging of the infection pathway of an adeno-associated virus. Science 294, 1929–1932.

Seksek, O., Biwersi, J., Verkman, A.S., 1997. Translational diffusion of macromolecule-sized solutes in cytoplasm and nucleus. J. Cell Biol. 138, 131–142.

Sodeik, B., Ebersold, M.W., Helenius, A., 1997. Microtubule-mediated transport of incoming herpes simplex virus 1 capsids to the nucleus. J. Cell Biol. 136, 1007–1021.

Stidwell, R.P., Greber, U.F., 2000. Intracellular virus trafficking reveals physiological characteristics of cytoskeleton. News Physiol. Sci. 15, 67–71.

Suomalainen, M., Nakano, M.Y., Keller, S., Boucke, K., Stidwill, R.P., Greber, U.F., 1999. Microtubule-dependent plus- and minus end-directed motilities are competing processes for nuclear targeting of adenovirus. J. Cell Biol. 144, 657–672.

Volkman, L.E., Goldsmith, P.A., 1985. Mechanism of neutralization of budded *Autographa californica* nuclear polyhedrosis virus by a monoclonal antibody: inhibition of entry by adsorptive endocytosis. Virology 143, 143–185.

Volkman, L.E., Zaal, K.J., 1990. *Autographa californica* M nuclear polyhedrosis virus: microtubules and replication. Virology 175 (1), 292–302.

Walss-Bass, C., Xu, K., David, S., Fellous, A., Ludueña, R.F., 2002. Occurrence of nuclear beta(II)-tubulin in cultured cells. Cell Tissue Res. 308, 215–223.

Ward, B.M., Moss, B., 2004. Vaccinia virus A36R membrane protein provides a direct link between intracellular enveloped virions and the microtubule motor kinesin. J. Virol. 78, 2486–2493.

Williams, G.V., Faulkner, P., 1997. Cytological changes and viral morphogenesis during baculovirus infection. In: Miller, L.K. (Ed.), The Baculoviruses. Plenum Press, New York, pp. 61–107.

Yang, P., Sampson, H.M., Krause, H.M., 2006. A modified tandem affinity purification strategy identifies cofactors of the *Drosophila* nuclear receptor dHNF4. Proteomics 6, 927–935.

Yeh, I.T., Ludueña, R.F., 2004. The betaII isotype of tubulin is present in the cell nuclei of a variety of cancers. Cell Motil. Cytoskelet. 57, 96–106.